

Surface-Compartmentalized Micelles by Stereocomplex-Driven Self-Assembly

Roman Schaller, Christian Hils, Matthias Karg, and Holger Schmalz*

The unique corona structure of surface-compartmentalized micelles (Janus micelles, patchy micelles) opens highly relevant applications, e.g. as efficient particulate surfactants for emulsion stabilization or compatibilization of polymer blends. Here, stereocomplex-driven self-assembly (SCDSA) as a facile route to micelles with a semicrystalline stereocomplex (SC) core and a patch-like microphase separated corona, employing diblock copolymers with enantiomeric poly(*L*-lactide)/poly(*D*-lactide) blocks and highly incompatible corona-forming blocks (polystyrene (PS), poly(*tert*-butyl methacrylate)) is introduced. The spherical patchy SC micelles feature a narrow size distribution and show a compartmentalized, shamrock-like corona structure. Compared to SC micelles with a homogeneous PS corona the patchy micelles have a significantly higher interfacial activity attributable to the synergistic combination of an amphiphilic corona with the Pickering effect of nanoparticles. The patchy micelles are successfully employed in the stabilization of emulsions, underlining their application potential.

coatings, and many more.^[1–7] In general, they can be divided into Janus micelles,^[8–13] featuring two opposing faces with different chemistry and/or polarity, and patchy micelles that are characterized by a patch-like microphase-separated corona consisting of several compartments. For the preparation of one-dimensional (cylindrical/worm-like) patchy micelles crystallization-driven self-assembly (CDSA) has proven an highly efficient method.^[14–22] However, other micelle shapes, like spherical patchy micelles, have only scarcely been reported yet. Besides, the formation of semicrystalline stereocomplexes (SC) between block copolymers bearing enantiomeric poly(*L*-lactide) (PLLA) and poly(*D*-lactide) (PDLA) blocks is a strong driving force for the formation of stable micelles (stereocomplex-driven self-assembly (SCDSA)).^[23,24] SC crystals consist of a parallel packing of PLLA 3₂ and PDLA 3₁ helices and feature an about 50 °C higher

1. Introduction


Surface-compartmentalized micelles are of substantial interest, as their unique corona structure opens a multitude of highly relevant applications, e.g. as efficient stabilizers for emulsions and polymer blends, in catalysis, as optical nanoprobe and biosensors, for self-propulsion, superhydrophobic and anti-ice

melting point compared to that of PLLA/PDLA homopolymers and are insoluble even in the solvents they have been prepared.^[25] The by far most studied SC micelles are based on linear block copolymers (AB-, ABA- and ABC-type), star-shaped block copolymers and graft copolymers with poly(ethylene oxide) (PEO) or poly(oligo(ethylene glycol) methacrylate) blocks rendering the SC micelles water soluble.^[26–29] Alternatively, block copolymers with poly(acrylic acid),^[30,31] poly(*N,N*-dimethylaminoethyl methacrylate)^[32] or poly(*isoglycerol* methacrylate)^[33] blocks were used. In contrast, only a few reports address SC micelle formation in organic solvents.^[34–36] Up to now there is only one report on SC micelles with a patchy poly(*N*-isopropyl acrylamide) (PNiPAAm)/PEO corona prepared by SCDSA in water.^[37] However, the cloud point of the PNiPAAm block was about 20 °C and, thus, the patchy corona structure was induced by a partial collapse of PNiPAAm.

Herein, we report on the preparation of spherical patchy micelles by SCDSA of diblock copolymers bearing enantiomeric PLLA and PDLA core-forming blocks and highly incompatible corona-forming blocks, namely PS-*b*-PLLA and P*t*BMA-*b*-PDLA (PS = polystyrene, P*t*BMA = poly(*tert*-butyl methacrylate)), in organic solvents (Scheme 1A). Next to the preparation and characterization of the spherical patchy SC micelles also their interfacial activity and potential as particulate surfactants will be addressed.

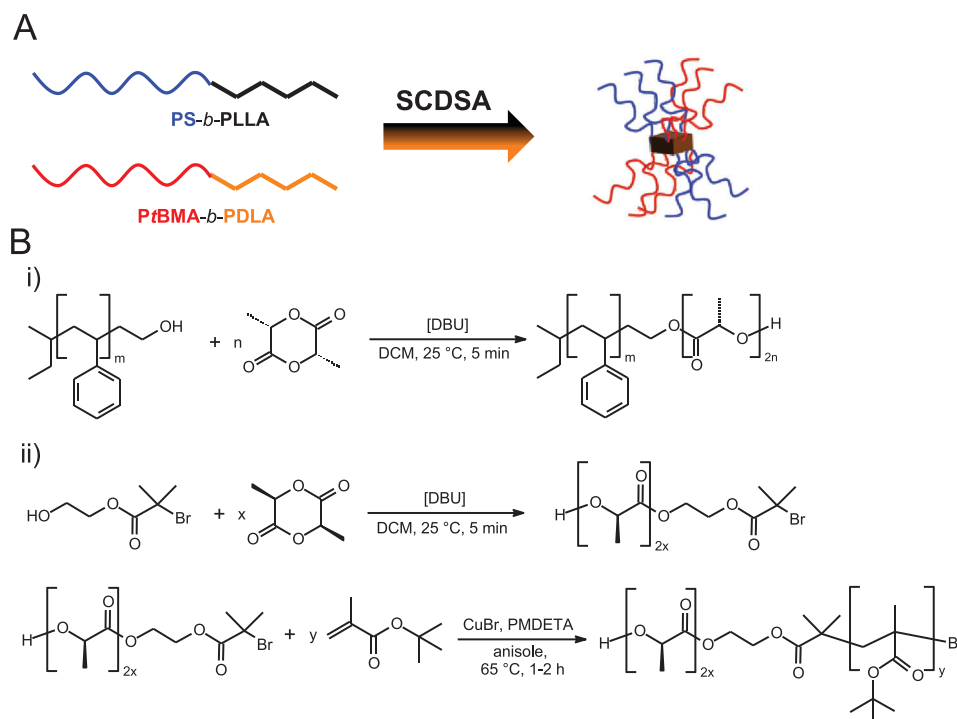
R. Schaller, C. Hils, H. Schmalz
 Macromolecular Chemistry II
 University of Bayreuth
 Universitätsstraße 30, 95447 Bayreuth, Germany
 E-mail: holger.schmalz@uni-bayreuth.de

M. Karg
 Physical Chemistry I / Colloids and Nanooptics
 Heinrich-Heine-University Düsseldorf
 Universitätsstraße 1, 40225 Düsseldorf, Germany
 H. Schmalz
 Bavarian Polymer Institute
 Universitätsstraße 30, 95447 Bayreuth, Germany

 The ORCID identification number(s) for the author(s) of this article can be found under <https://doi.org/10.1002/marc.202200682>

© 2022 The Authors. Macromolecular Rapid Communications published by Wiley-VCH GmbH. This is an open access article under the terms of the Creative Commons Attribution License, which permits use, distribution and reproduction in any medium, provided the original work is properly cited.

DOI: 10.1002/marc.202200682



Scheme 1. A) Concept for the preparation of patchy micelles via SCDSA and B) synthesis of diblock copolymers.

2. Results and Discussion

2.1. SCDSA of Diblock Copolymer Mixtures to Spherical Patchy Micelles

The used PS-*b*-PLLA diblock copolymer ($S_{169}LLA_{119}$, subscripts denote number-averaged degrees of polymerization) was synthesized by organo-catalyzed ring-opening polymerization (ROP) of *L*-lactide starting from a PS-OH macroinitiator prepared by anionic polymerization of styrene and end-capping with ethylene oxide (Scheme 1B,i)). For the synthesis of PtBMA-*b*-PDLA ($tBMA_{172}DLA_{114}$) a combination of ROP of *D*-lactide with atom transfer radical polymerization of *t*BMA was employed, utilizing 2-hydroxyethyl 2-bromoisobutyrate as bifunctional initiator (Scheme 1B,ii)). Details on synthesis and molecular characterization of the diblock copolymers can be found in the Experimental Section and Supporting Information (Figure S1, S2 and Table S1, Supporting Information). For the preparation of patchy SC micelles the diblock copolymers were first dissolved in dichloromethane (DCM, $c = 10 \text{ g L}^{-1}$) as non-selective solvent, employing a 1/1 (*w/w*) ratio with respect to the enantiomeric PLA blocks. A PLLA/PDLA ratio of 1/1 (*w/w*) was chosen to ensure an equimolar ratio of the enantiomeric PLA units for efficient SC formation. Then, the mixture ($V = 300 \mu\text{L}$) was added drop-wise to an excess of cyclohexane (CH, $V = 3 \text{ mL}$), a selective solvent for the PS and PtBMA corona-forming blocks, under stirring to induce SC formation and crystallization followed by aging for at least 1 day at ambient conditions (no stirring was applied during aging). This resulted in a dispersion of PS-*sc*-PLA-PtBMA micelles ($c = 0.9 \text{ g L}^{-1}$ in CH/DCM = 10/1 (*v/v*)) with an insoluble SC core and a soluble PS/PtBMA corona. Dynamic light scatter-

ing (DLS) revealed a narrow size distribution of the SC micelles with an apparent hydrodynamic diameter of $D_{h,\text{app}} = 104 \pm 30 \text{ nm}$ (Figure 1A). In the beginning, the micelle size increases slightly with time and stays constant after ca. 6 h (Figure 1B). The mean diameter and the diameter distribution do not change significantly even after ten weeks of aging. This underlines the stability of the SC micelles in dispersion (Figure S3A, Supporting Information). Also the time between preparing the diblock copolymer mixture in DCM and SCDSA in CH has no obvious impact on the size distribution of the micelles (Figure S3B, Supporting Information).

From the transmission electron microscopy (TEM) micrograph shown in Figure 1C a patch-like microphase-separated corona of the micelles can be clearly deduced. Due to selective staining with RuO_4 vapor PS domains appear dark and the semicrystalline PLA SC core as well as the PtBMA domains in the corona bright. The micelles feature different numbers of PS patches, mostly 3–5, and hence the micelle structure might be described best as a shamrock-like morphology. The patchy corona structure becomes even clearer by comparison with PS-*sc*-PLA-PS micelles prepared by SCDSA of $S_{169}LLA_{119}$ and $S_{169}DLA_{190}$ under identical conditions. The micelles exhibit a narrow size distribution with a comparable $D_{h,\text{app}}$ of $82 \pm 25 \text{ nm}$ (Figure 1A) and from TEM (Figure 1D) the difference in corona structure is evident, appearing now homogeneously dark. As DLS shows narrow size distributions the observed agglomeration of the SC micelles on the TEM grid can be attributed to drying artifacts arising from sample preparation. CDSA of the individual diblock copolymers under identical conditions as employed for SCDSA resulted in crystalline-core (PLLA or PDLA) micelles with increased sizes, broader size distributions and mostly cylindrical shapes (Figure

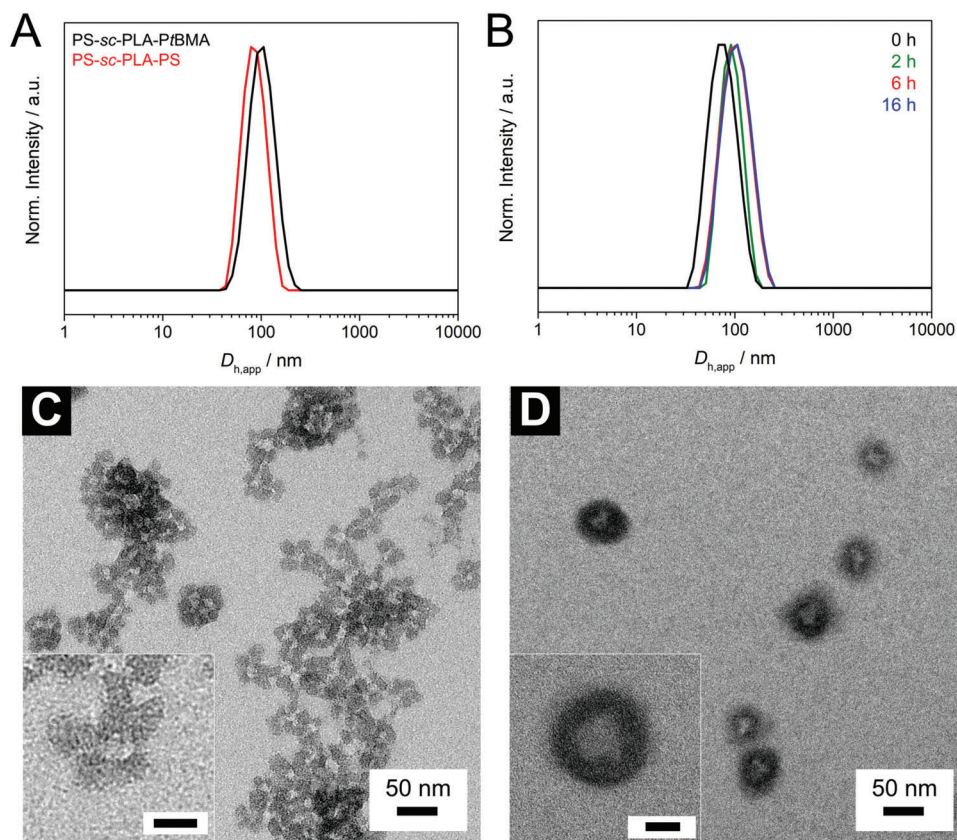


Figure 1. Hydrodynamic diameter distributions from DLS for A) SC micelles prepared from PS-*b*-PLLA/*Pt*BMA-*b*-PDLA and PS-*b*-PLLA/PS-*b*-PDLA mixtures, respectively ($c = 0.9 \text{ g L}^{-1}$, CH/DCM = 10/1 (v/v)), and B) of a PS-*sc*-PLA-*Pt*BMA micelle dispersion after aging for different times as indicated. TEM micrographs (RuO₂ staining, scale bars inset = 20 nm) of the corresponding SC micelles with C) a patchy PS/*Pt*BMA corona and D) a homogeneous PS corona. The small black dots in the PS patches are RuO₂ nanoparticles, which form selectively in the PS domains during the staining process.

S4, Supporting Information). This indicates that the formation of spherical patchy micelles from the diblock copolymer mixtures is solely driven by SC formation.

In the Raman spectra of the SC micelles with a patchy PS/*Pt*BMA as well as homogeneous PS corona a shift of the carbonyl stretching vibration from $\approx 1771 - 1773 \text{ cm}^{-1}$ for the individual diblock copolymers to $\approx 1752 - 1755 \text{ cm}^{-1}$ is observed (Figure 2). This characteristic shift to lower wavenumbers proves that self-assembly is indeed driven by SC formation between the enantiomeric PLLA/PDLA blocks.^[23,34,36,38,39] Nevertheless, the carbonyl band does not shift completely to lower wavenumbers, indicating that some lactide units (probably at the core/corona interface) did not take part in SC formation.

As a comparison, the respective diblock copolymer mixtures in DCM were directly precipitated in *n*-pentane, a non-solvent for all blocks. The obtained solids upon precipitation were studied by Raman spectroscopy. Interestingly, for the PS-*sc*-PLA-*Pt*BMA micelles the SC specific band at about 1755 cm^{-1} is more pronounced with respect to the sample prepared by precipitation in *n*-pentane, pointing to a more efficient SC formation upon SCDSA in CH. For PS-*sc*-PLA-PS no significant difference between both methods was observed. These results show that SC formation is a very fast process as even upon direct precipitation SCs are formed. In addition, differential scanning calorimetry revealed significantly higher melting temperatures for the

SC micelles ($T_m \approx 200 \text{ }^\circ\text{C}$) with respect to that observed for the neat PLLA and PDLA homopolymers ($T_m \approx 145 \text{ }^\circ\text{C}$), further underlining that SC formation and crystallization is the driving force for self-assembly (Figure S6, S7; Table S2, Supporting Information).^[25,38,39] It is noted that PLLA or PDLA related melting transitions were not observed for the employed PS-*b*-PLLA and *Pt*BMA-*b*-PDLA diblock copolymers due to confinement effects (Figure S6, Supporting Information).^[40] The degree of SC crystallization was determined to $\alpha = 34\%$ for PS-*sc*-PLA-*Pt*BMA and $\alpha = 31\%$ for PS-*sc*-PLA-PS (Table S2, Supporting Information), which is in accordance with Raman results revealing the presence of PLLA/PDLA units that did not take part in SC formation. Accordingly, about 70% of the micellar core is still amorphous allowing the PS and *Pt*BMA corona chains to self-assemble into distinct nanometer-sized patches, as otherwise the parallel packing of PLLA and PDLA blocks in the SC crystal might hamper the segregation of the corona chains for higher degrees of crystallinity.

2.2. Effect of Dilution on Micelle Size and Corona Structure

Next, we studied whether dilution has an impact on the structure of the SC micelles, keeping the concentration of the diblock copolymer mixture in DCM constant at $c = 10 \text{ g L}^{-1}$. Accordingly,

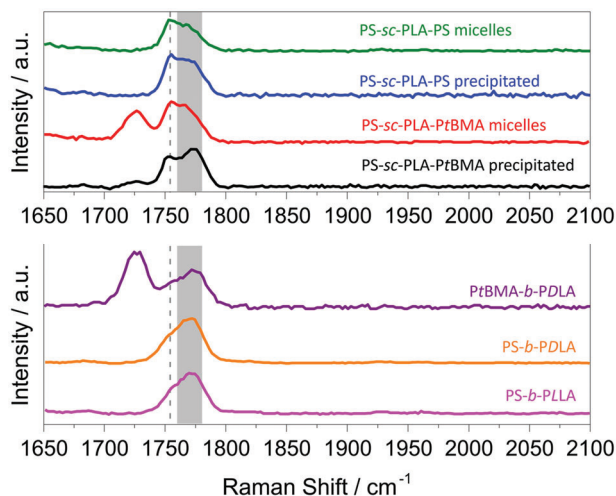


Figure 2. Raman spectra of employed diblock copolymers, dried SC micelles, and solid SCs prepared by direct precipitation of the diblock copolymer mixtures in DCM into *n*-pentane. Shown are zoom-ins of the carbonyl stretching vibration regime (dashed line indicates location of SC specific band, full spectra are given in Figure S5, Supporting Information).

smaller amounts of the diblock copolymer mixtures ($V = 60$ and $30 \mu\text{L}$), prepared in an identical manner as described above, were added in one portion to 3 mL of CH and aged for 1 day. This yielded SC micelle dispersions with a concentration of $c = 0.2 \text{ g L}^{-1}$ in CH/DCM = 50/1 (v/v) and $c = 0.1 \text{ g L}^{-1}$ in CH/DCM = 100/1 (v/v), respectively. DLS again shows narrow size distributions for the formed SC micelles at $c = 0.2 \text{ g L}^{-1}$ (Figure S8A, Supporting Information; PS-*sc*-PLA-*Pt*BMA: $D_{h,app} = 50 \pm 14 \text{ nm}$) as well as $c = 0.1 \text{ g L}^{-1}$ (Figure 3A; PS-*sc*-PLA-*Pt*BMA: $D_{h,app} = 52 \pm 17 \text{ nm}$, PS-*sc*-PLA-PS: $D_{h,app} = 50 \pm 14 \text{ nm}$), however, being significantly smaller compared to the micelles prepared at lower dilution (Figure 1A). The smaller size of the micelles might be attributed to the altered preparation method employed. For higher dilutions (CH/DCM = 50/1 and 100/1 (v/v)) small amounts of the diblock copolymer mixtures in DCM were added in one portion to CH in contrast to the drop-wise addition employed for lower dilution (CH/DCM = 10/1 (v/v)).

Since SC formation is a very fast process, as revealed from the samples prepared by direct precipitation in *n*-pentane (Figure 2, S7; Table S2, Supporting Information), SC micelles are formed instantaneously upon addition of the DCM solution to CH. This is confirmed by the observation that the size

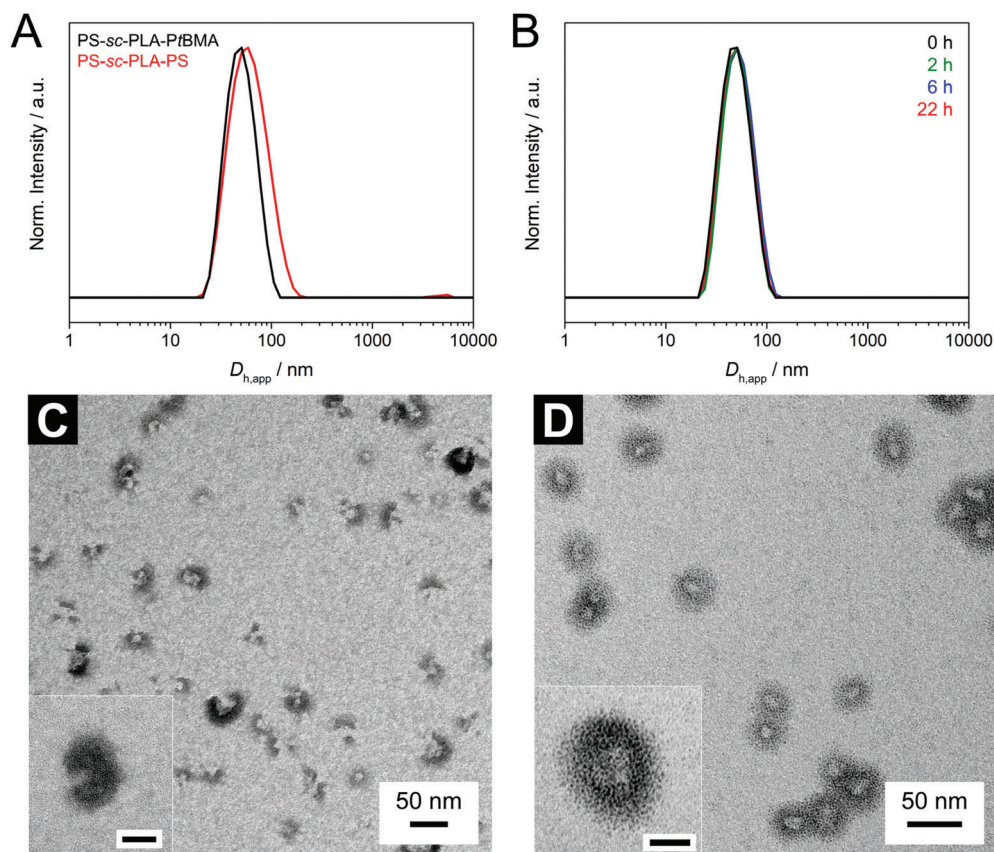


Figure 3. Hydrodynamic diameter distributions from DLS for A) SC micelles prepared from PS-*b*-PLLA/*Pt*BMA-*b*-PDLA and PS-*b*-PLLA/PS-*b*-PDLA mixtures, respectively, and B) of a PS-*sc*-PLA-*Pt*BMA micelle dispersion after aging for different times as indicated, employing a higher dilution ($c = 0.1 \text{ g L}^{-1}$, CH/DCM = 100/1 (v/v)). TEM micrographs of the formed SC micelles (RuO_4 staining, scale bars inset = 20 nm) with C) a surface-compartmentalized PS/*Pt*BMA and D) a homogeneous PS corona.

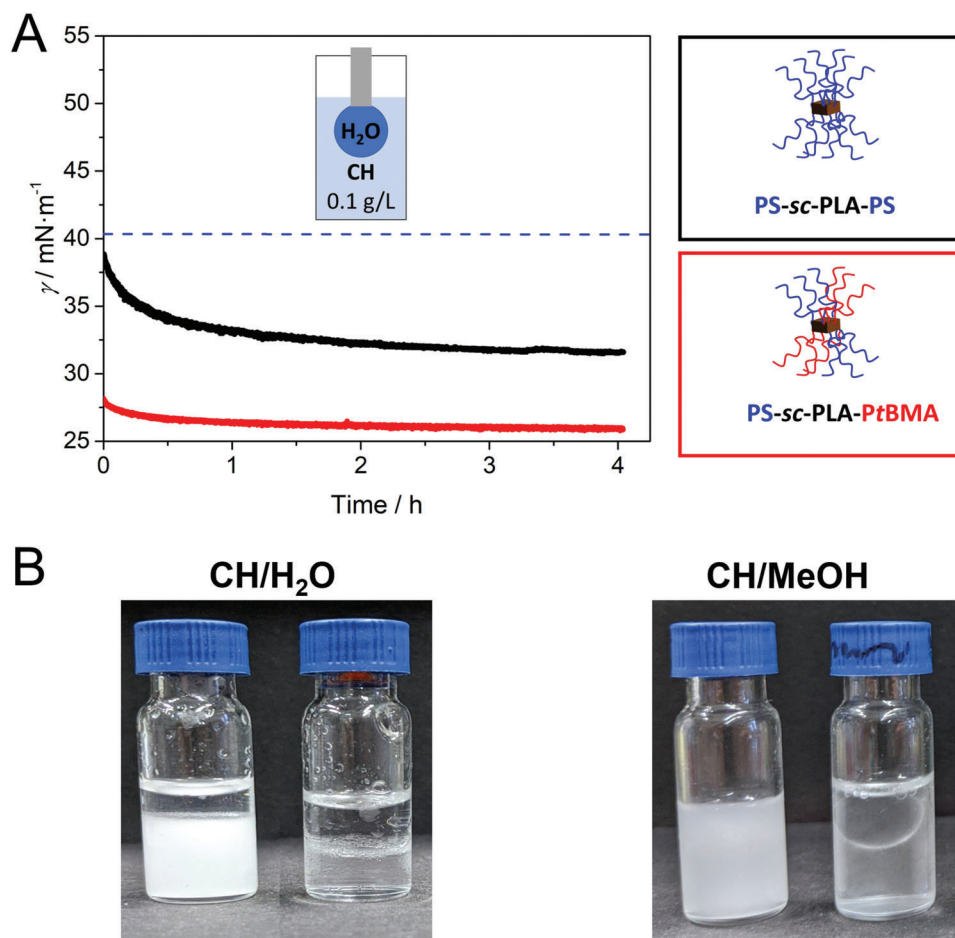


Figure 4. A) Interfacial tension isotherms of spherical PS-*sc*-PLA-*Pt*BMA micelles with a patchy corona compared to spherical PS-*sc*-PLA-PS micelles with a homogeneous corona at the CH/water interface. The dashed blue line is the interfacial tension at the pristine CH/water interface measured as reference. B) CH/water and CH/methanol mixtures emulsified with patchy PS-*sc*-PLA-*Pt*BMA micelles ($c = 0.9 \text{ g L}^{-1}$ in CH). The photographs on the right of each mixture correspond to the respective pure solvent mixtures that separated immediately after shaking.

distribution of the micelles formed at CH/DCM = 100/1 (v/v) (Figure 3B) does not change with time in contrast to the behavior at lower dilution (CH/DCM = 10/1 (v/v), Figure 2B) and that the degree of stereocomplexation as deduced from Raman spectroscopy is comparable (Figure S9, Supporting Information). Accordingly, during the drop-wise addition SC micelles are presumably formed instantaneously upon addition of the first drop and micelles grow with time during further addition and subsequent aging. This in turn indicates the presence of a certain amount of unimers in solution that can add to the SC micelles, which might be facilitated by the comparably high DCM content (non-selective solvent) of 9 vol.% for the samples prepared at lower dilution.

Interestingly, the corona of the PS-*sc*-PLA-*Pt*BMA micelles prepared at higher dilutions (Figure S8B, Supporting Information: CH/DCM = 50/1 (v/v), Figure 3C: CH/DCM = 100/1 (v/v)) exhibits some distinct differences with respect to the quite uniform patchy structure observed before (Figure 1C). Here, a mixture of SC micelles with a patchy and a Janus-like corona structure is formed instead, both featuring defined compartments in the

corona. If the Janus-type micelles are oriented in a proper way on the carbon-coated copper grid (inset Figure 3C), they can be distinguished as micelles with a bright appearing PLA SC core, which is surrounded by a dark PS and a bright *Pt*BMA hemisphere. In contrast, if one side of the micelle is facing the surface of the grid (preferentially the PS face), the micelle corona appears homogeneously dark. The concomitant formation of Janus micelles might be attributed to the significantly lower micelle size, which favors to some extent a separation into two distinct PS and *Pt*BMA faces due to a denser chain packing and, hence, increased segregation strength in the corona. Also the reduced DCM amount in the dispersions prepared at higher dilutions (2 vol.% for CH/DCM = 50/1 (v/v) and 1 vol.% for CH/DCM = 100/1 (v/v), respectively) might induce a somewhat higher incompatibility as DCM is a good solvent for both PS and *Pt*BMA, whereas CH (theta solvent for PS) is a slightly better solvent for *Pt*BMA. The PS-*sc*-PLA-PS micelles show again a homogeneously dark appearing PS corona (Figure 3D), being clearly distinguishable from the compartmentalized corona of the PS-*sc*-PLA-*Pt*BMA micelles.

2.3. Interfacial Activity of Spherical Patchy SC Micelles

To test the potential of the patchy PS-*sc*-PLA-*Pt*BMA micelles as particulate surfactants the interfacial tension at the CH/water interface was studied. To this end, the micelle dispersions ($c = 0.9 \text{ g L}^{-1}$, CH/DCM = 10/1 (v/v), Figure 1) were dialyzed against pure CH prior to the measurement and diluted to $c = 0.1 \text{ g L}^{-1}$. DLS and TEM shows that the size and corona structure of the micelles did not change upon dialysis (Figure S10, Supporting Information). Figure 4A reveals a significantly higher interfacial activity of the patchy micelles compared to SC micelles with a homogeneous PS corona, resulting in a decrease of the quasi-equilibrium interfacial tension to $\gamma = 25.9 \pm 0.1 \text{ mN m}^{-1}$ ($\gamma = 31.6 \pm 0.1 \text{ mN m}^{-1}$ for PS-*sc*-PLA-PS and $\gamma = 40.3 \pm 0.1 \text{ mN m}^{-1}$ for pristine CH/water interface). Notably, the decrease of interfacial tension in the beginning is steeper for the patchy micelles, which can be attributed to their pronounced interfacial activity promoted by the combination of an amphiphilic corona with the Pickering effect of nanoparticles.

Exemplarily, we have tested the potential of patchy PS-*sc*-PLA-*Pt*BMA micelles as particulate surfactants in the emulsification of CH/water and CH/methanol mixtures (50/50 (v/v)), employing dispersions with a concentration of $c = 0.9 \text{ g L}^{-1}$ (Figure 4B). For the CH/water mixture the emulsion sediments to the bottom of the vial and is overlaid with excess oil (CH) phase. As the density of water is significantly higher compared to that of CH ($\rho(\text{CH}) = 0.78 \text{ g cm}^{-3}$) a water-in-oil (w/o) emulsion is formed accordingly. This is in accordance with emulsification studies on Janus particles featuring two hydrophobic faces.^[41] In case of the CH/methanol mixture a homogeneous emulsion was obtained, which might be attributed to the comparable densities of both solvents ($\rho(\text{MeOH}) = 0.79 \text{ g cm}^{-3}$) in combination with methanol being a selective solvent for *Pt*BMA. Here, the PS patches are soluble in the CH phase and the *Pt*BMA patches in the methanol phase, respectively, in contrast to CH/water where both patches are insoluble in the water phase.

3. Conclusion

This work shows that SCDSA of diblock copolymers bearing enantiomeric PLLA and PDLA blocks as well as strongly incompatible, amorphous corona-forming blocks is a facile route toward spherical patchy micelles with excellent interfacial activity. This modular approach allows for an easy variation of corona-forming blocks and, thus, corona chemistries to tune interfacial activity or functionality. This might open interesting applications not only as efficient particulate surfactants/compatibilizers but also in other fields like heterogeneous catalysis or hierarchically structured assemblies.

4. Experimental Section

Materials: All chemicals were used as received unless otherwise noted. Ethylene oxide (Linde, 3.0) was condensed onto calcium hydride (CaH_2) and stirred at $0 \text{ }^\circ\text{C}$ for 3 h before being transferred into a storage ampoule. Prior to use ethylene oxide was additionally purified over *n*-butyllithium at $0 \text{ }^\circ\text{C}$. Styrene (>99%, Sigma-Aldrich) was stirred over *n*-butylmagnesium (Bu_2Mg) under nitrogen and condensed into a storage ampoule. Dichloromethane (DCM, $\geq 99.8\%$, analytical reagent grade, Thermo Scientific) used for lactide polymerization was stirred over CaH_2

and distilled. *n*-Pentane (technical grade) was purified by distillation prior to use. Tetrahydrofuran (THF, 99.9%, Sigma-Aldrich) was dried by successive distillation from CaH_2 and potassium and stored under nitrogen until use. 1,8-Diazabicyclo[5.4.0]undec-7-ene (DBU, >98%, TCI) was distilled from CaH_2 before use. *D*- and *L*-lactide ($\geq 99.8\%$, PURASORB D and L, Corbion, Amsterdam, The Netherlands) were recrystallized from toluene and stored under nitrogen or argon. *tert*-Butyl methacrylate (*t*BMA, BASF SE) was passed through a column with basic alumina and *N, N, N', N', N'*-pentamethyldiethylenetriamine (PMDETA, 99%, Sigma-Aldrich) was distilled prior to use. Deionized water (filtered through a Millipore Milli-Q Plus system, QPAK 2 purification cartridge, conductivity: $18.2 \text{ M}\Omega \text{ cm}$), Bu_2Mg (1.0 M in heptane, Sigma-Aldrich), *sec*-butyllithium (*sec*-BuLi, 1.3 M in cyclohexane/hexane, Thermo Scientific), *n*-butyllithium (*n*-BuLi, 1.6 M in hexanes, Thermo Scientific), benzoic acid (p.a., AlppiChem), copper(I) bromide (Cu(I)Br , 98%, Sigma-Aldrich), CaH_2 (Merck), 2-hydroxyethyl 2-bromoisobutyrate (HEBiB, 95%, Sigma-Aldrich), deuterated chloroform (CDCl_3 , 99.8%, Deutero), ruthenium(III) chloride hydrate (ReagentPlus, Sigma-Aldrich), sodium hypochlorite solution (NaOCl, 10–15 wt.% in water, Sigma-Aldrich), hydrochloric acid (HCl, 37 wt.% in water, VWR), cyclohexane (CH, $\geq 99.8\%$, analytical reagent grade, Thermo Scientific), anisole (>99%, Solvagreen, Th. Geyer), 1,4-dioxane ($\geq 99.8\%$, analytical reagent grade, Thermo Scientific), methanol (MeOH, $\geq 99.9\%$, analytical reagent grade, Thermo Scientific) and dialysis membrane (Spectra/Por® 1, molecular weight cut-off: 6000 – 8000 Dalton).

Synthesis of Hydroxy Terminated Polystyrene Macroinitiator (PS-OH): PS-OH was prepared by anionic polymerization of styrene in THF followed by end-capping with ethylene oxide. Polymerization of styrene was conducted at $-78 \text{ }^\circ\text{C}$ using *sec*-BuLi as initiator. After complete conversion a five-fold molar excess of ethylene oxide was added for end-capping followed by stirring for 30 min. The polymer was terminated with a mixture of acetic acid/methanol (1/5 (v/v)) and isolated by precipitation from methanol. The product was filtered and dried in vacuo ($20 \times 10^{-3} \text{ mbar}$) at $40 \text{ }^\circ\text{C}$.

Synthesis of D-Lactide Based ATRP Macroinitiator: PDLA-ATRP was prepared according to the literature under an inert argon atmosphere.^[42] To *D*-lactide in DCM ($c \approx 150 \text{ g L}^{-1}$) a solution of HEBiB (380 μL , 0.41 mmol, $c = 1.07 \text{ mol L}^{-1}$ in DCM) was added at room temperature. DBU (4 eq with respect to HEBiB) was added and the reaction mixture was stirred for 5 min. Subsequently, the reaction was stopped by the addition of benzoic acid (equimolar amount to DBU) and the mixture was stirred for 30 min. The product was precipitated from *n*-pentane/MeOH (10/1 (v/v)), filtrated and dried in vacuo ($5 \times 10^{-6} \text{ mbar}$).

Synthesis of PS-*b*-PLLA and PS-*b*-PDLA: PS-*b*-PLLA and PS-*b*-PDLA were prepared according to the literature.^[42] To PS-OH in DCM ($c \approx 150 \text{ g L}^{-1}$) the respective *L*- or *D*-lactide was added and stirred at room temperature for 10 min under argon. DBU (4 eq with respect to OH end groups) was added and the reaction mixture was stirred for 5 min. Subsequently, benzoic acid (equimolar amount to DBU) was added to stop the reaction and the mixture was stirred for 30 min. The products were precipitated from *n*-pentane/MeOH (10/1 (v/v)), filtrated and dried in vacuo ($5 \times 10^{-6} \text{ mbar}$).

Synthesis of *Pt*BMA-*b*-PDLA: *Pt*BMA-*b*-PDLA was prepared according to the literature.^[43,44] PDLA-ATRP (1.0 g), *t*BMA (8.0 mL) and PMDETA (50.9 μL) were mixed together in anisole (15 mL) and degassed with argon for 60 min. The solution was heated to $65 \text{ }^\circ\text{C}$ and Cu(I)Br (35.0 mg) was added under stirring. The employed molar ratio of macroinitiator/ Cu(I)Br /PMDETA was 1/2/2. After 130 min the reaction was quenched by placing the mixture into liquid nitrogen. The reaction mixture was passed through a neutral alumina column to remove the catalyst. The product was precipitated from $\text{H}_2\text{O}/\text{MeOH}$ (2/1 (v/v)), filtrated and dried in vacuo ($5 \times 10^{-6} \text{ mbar}$). Finally, the diblock copolymer was dissolved in 1,4-dioxane and freeze-dried to yield a white powder.

Preparation of PLA Stereocomplexes via Precipitation: Typically, solutions of PLA homopolymers or PLA based diblock copolymers in DCM ($c = 10 \text{ g L}^{-1}$) were mixed together, employing a 1/1 weight ratio with respect to the enantiomeric PLLA/PDLA blocks. The mixtures were precipitated from *n*-pentane (combination of PLLA-ATRP/PDLA-ATRP, PS-*b*-PLLA/PS-

b-PDLA) or H₂O/MeOH (2/1 (ν/ν), combination of PS-*b*-PLLA/PtBMA-*b*-PDLA), respectively. After removal of the solvents by evaporation or separation by centrifugation the obtained white solids were dried in vacuo (5×10^{-6} mbar). These samples prepared by direct precipitation are denoted as PS-*sc*-PLA-PtBMA precipitated or PS-*sc*-PLA-PS precipitated, respectively.

SCDSA of Diblock Copolymer Mixtures: Solutions of PS-*b*-PLLA and PtBMA-*b*-PDLA in DCM ($c = 10 \text{ g L}^{-1}$) were mixed together, employing a 1/1 weight ratio with respect to the enantiomeric PLA blocks. In a 5 mL snap lid vial, equipped with a small magnetic stirring bar, the obtained mixture (300 μL) was added dropwise to CH (3 mL) over 20 sec while stirring (approximately 700 rpm), resulting in a micelle dispersion with a concentration of $c = 0.9 \text{ g L}^{-1}$ and a final solvent ratio of CH/DCM = 10/1 (ν/ν). Subsequently, the dispersion was stirred for an additional 1 min and then aged at room temperature without stirring for at least one day before DLS and TEM characterization. The same protocol was applied to the combination of PS-*b*-PLLA and PS-*b*-PDLA starting from solutions with concentrations of $c = 10 \text{ g L}^{-1}$. Analogously, micelle dispersions with concentrations of $c = 0.2$ and 0.1 g L^{-1} and final solvent ratios of CH/DCM = 50/1 and 100/1 (ν/ν), respectively, were prepared by adding smaller amounts of the diblock copolymer mixture in DCM (60 and 30 μL , $c = 10 \text{ g L}^{-1}$) in one portion to the same volume of CH (3 mL) using a micropipette. The dispersion of SC micelles prepared by SCDSA are denoted as PS-*sc*-PLA-PtBMA micelles or PS-*sc*-PLA-PS micelles, respectively.

CDSA of Neat Diblock Copolymers: CDSA of the individual diblock copolymers in C was conducted the same way as described above for SCDSA of diblock copolymer mixtures, starting from DCM solutions of the diblock copolymers with concentrations of $c = 10 \text{ g L}^{-1}$.

Characterization Techniques: The polymers were characterized by proton nuclear magnetic resonance (¹H NMR) spectroscopy using a Bruker Ultrashield-300 spectrometer (300 MHz) at 20 °C. The chemical shift (δ) was determined relatively to the signal of the solvent CDCl₃ (δ (¹H) = 7.26 ppm).

Size exclusion chromatography (SEC) was performed on a SEC 1260 Infinity system (Agilent Technologies, Santa Clara, CA, USA) with two PSS-SDV gel columns (particle size = 5 μm) with porosity range from 10^2 to 10^5 Å (PSS, Mainz, Germany). CHCl₃ (HPLC grade) was used as eluent. All samples were dissolved and filtered through a 0.2 μm PTFE filter before analyses. The samples were measured at a flow rate of 0.5 mL min^{-1} at 23 °C, using a refractive index detector (Agilent Technologies, Santa Clara, CA, USA). A calibration with narrowly distributed PS standards (PSS calibration kit) and toluene (HPLC grade) as internal standard were used.

A confocal WITec Alpha 300 RA+ Raman imaging system equipped with a UHTS 300 spectrometer and a back-illuminated Andor Newton 970 EM-CCD camera together with the WITec Suite FIVE 5.3 software package was employed for Raman measurements. All spectra were acquired with an excitation wavelength of $\lambda = 532 \text{ nm}$ and a 50x long working distance objective (Zeiss LD EC Epiplan-Neofluar Dic 50x, NA = 0.55). Typically, a laser intensity of 20 mW and integration times of 0.5–1 s (grating: 600 g mm^{-1}) were employed and 50 measurements were accumulated for a spectrum. All spectra were corrected for cosmic ray spikes and subjected to a background removal routine. Samples of the micelle dispersions were prepared by dropping small amounts ($3 \times 5 \mu\text{L}$) of the dispersion onto a glass slide followed by drying in vacuo (3 h, 20 mbar).

Differential scanning calorimetry (DSC) was performed on a Mettler Toledo DSC 3+ or a Netzsch DSC 204 F1 Phoenix instrument using aluminum crucibles (pierced lid) and nitrogen as protecting gas. The temperature range was selected from -20 °C to 220 °C employing a scanning rate of 10 K min^{-1} .

Dynamic light scattering (DLS) was conducted on a Zetasizer Nano S (Malvern Panalytical, UK) instrument equipped with a red He-Ne laser ($\lambda = 632.8 \text{ nm}$) and a detector placed at $\theta = 173^\circ$ to the incident radiation. The micelle dispersions were measured without further dilution at 25 °C in quartz glass cuvettes (10.0 mm path length), which were sealed with Teflon tape to prevent solvent evaporation. Data analyses were carried out using the Malvern Zetasizer software (version 7.13). The results are displayed as normalized intensity weighted size distributions and micelle sizes are reported as apparent hydrodynamic diameter ($D_{h,app}$) determined from the average of three replicate measurements.

Transmission electron microscopy (TEM) was carried out with a Zeiss CEM902 and a Zeiss/LEO EM922 Omega TEM. All microscopes are energy filtering transmission electron microscopes (EFTEMs), operated at an acceleration voltage of 80 kV and 160/200 kV, respectively. Zero-loss filtered micrographs ($\Delta E \approx 0 \text{ eV}$) were taken with a side mounted CCD camera system (Orius, Gatan) in case of the Zeiss CEM902 and a bottom mounted CCD camera (Ultrascan 1000, Gatan) in case of the Zeiss/LEO EM922 Omega, respectively. The images were processed with a digital image processing software (Digital Micrograph DM 1.9, DM 2.3, Gatan). For TEM analyses of the micelle dispersions, samples were diluted to a concentration of $c = 0.1 \text{ g L}^{-1}$ and stirred for 30 min at room temperature. Subsequently, 10 μL of the respective dispersion was applied to a carbon-coated copper grid and residual solvent was removed directly by blotting with a filter paper followed by drying of the coated copper grid under vacuum (24 h, 1×10^{-5} mbar, room temperature). For RuO₄ staining the samples were treated for 7–12 min with RuO₄ vapor, which was formed in situ from RuCl₃ hydrate and NaOCl. After staining, the samples were stored for at least 1 h in a fume hood to ensure that any not reacted RuO₄ was completely removed.

Interfacial tension measurements were performed using a DS25 from Krüss. The interfacial tensions at the CH/water interface were determined with the software “Advanced Drop Shape Analyses” (version 1.3.1.0) and the method “Pendant Drop” employing a droplet volume of $V = 20 \mu\text{L}$ (deionized water). Micellar dispersions were measured at a concentration of $c = 0.1 \text{ g L}^{-1}$. The quasi-equilibrium interfacial tensions were determined as average over the last 30 min of the respective measurement, where the interfacial tension levels off. The interfacial tension of the pristine CH/water interface was determined to $\gamma = 40.3 \text{ mN m}^{-1}$.

Supporting Information

Supporting Information is available from the Wiley Online Library or from the author.

Acknowledgements

Financial support by the German Research Foundation (project SCHM2428/3-1) is gratefully acknowledged. The authors thank A. Greiner for helpful discussions, M. Drechsler for help with TEM measurements and Rika Schneider for SEC measurements. The authors acknowledge support from the Keylabs Electron and Optical Microscopy and Synthesis and Molecular Characterization of the Bavarian Polymer Institute (BPI) at the University of Bayreuth and Corbion for the donation of *D*- and *L*-lactide.

Open access funding enabled and organized by Projekt DEAL.

Conflict of Interest

The authors declare no conflict of interest.

Data Availability Statement

The data that support the findings of this study are available in the supplementary material of this article.

Keywords

block copolymers, crystallization-driven self-assembly, particulate surfactants, patchy micelles, stereocomplexes

Received: August 10, 2022

Revised: October 11, 2022

Published online: November 6, 2022

- [1] A. H. Gröschel, A. H. E. Müller, *Nanoscale* **2015**, 7, 11841.
- [2] M. Karayianni, S. Pispas, *J. Polym. Sci.* **2021**, 59, 1874.
- [3] Y. Lu, J. Lin, L. Wang, L. Zhang, C. Cai, *Chem. Rev.* **2020**, 120, 4111.
- [4] A. K. Pearce, T. R. Wilks, M. C. Arno, R. K. O'Reilly, *Nat. Rev. Chem.* **2021**, 5, 21.
- [5] U. Tritschler, S. Pearce, J. Gwyther, G. R. Whittell, I. Manners, *Macromolecules* **2017**, 50, 3439.
- [6] M. Vafaezadeh, W. R. Thiel, *Angew. Chem., Int. Ed.* **2022**, 61, e202206403.
- [7] J. Du, R. K. O'Reilly, *Chem. Soc. Rev.* **2011**, 40, 2402.
- [8] A. Walther, A. H. E. Müller, *Chem. Rev.* **2013**, 113, 5194.
- [9] Q. Yang, K. Loos, *Polym. Chem.* **2017**, 8, 641.
- [10] X. Fan, J. Yang, X. J. Loh, Z. Li, *Macromol. Rapid Commun.* **2019**, 40, 1800203.
- [11] R. Deng, F. Liang, J. Zhu, Z. Yang, *Mater. Chem. Front.* **2017**, 1, 431.
- [12] G. Agrawal, R. Agrawal, *ACS Appl. Nano Mater.* **2019**, 2, 1738.
- [13] T. Pelras, C. S. Mahon, M. Müllner, *Angew. Chem., Int. Ed.* **2018**, 57, 6982.
- [14] C. Hils, I. Manners, J. Schöbel, H. Schmalz, *Polymers* **2021**, 13, 1481.
- [15] S. Song, X. Liu, E. Nikbin, J. Y. Howe, Q. Yu, I. Manners, M. A. Winnik, *J. Am. Chem. Soc.* **2021**, 143, 6266.
- [16] J. Schöbel, M. Karg, D. Rosenbach, G. Krauss, A. Greiner, H. Schmalz, *Macromolecules* **2016**, 49, 2761.
- [17] J. R. Finnegan, D. J. Lunn, O. E. C. Gould, Z. M. Hudson, G. R. Whittell, M. A. Winnik, I. Manners, *J. Am. Chem. Soc.* **2014**, 136, 13835.
- [18] A. M. Oliver, J. Gwyther, M. A. Winnik, I. Manners, *Macromolecules* **2018**, 51, 222.
- [19] S. Ganda, M. H. Stenzel, *Prog. Polym. Sci.* **2020**, 101, 101195.
- [20] L. MacFarlane, C. Zhao, J. Cai, H. Qiu, I. Manners, *Chem. Sci.* **2021**, 12, 4661.
- [21] J. Xu, H. Zhou, Q. Yu, I. Manners, M. A. Winnik, *J. Am. Chem. Soc.* **2018**, 140, 2619.
- [22] J. Schmelz, M. Karg, T. Hellweg, H. Schmalz, *ACS Nano* **2011**, 5, 9523.
- [23] H. Tsuji, *Adv. Drug Delivery Rev.* **2016**, 107, 97.
- [24] Z. Li, B. H. Tan, T. Lin, C. He, *Prog. Polym. Sci.* **2016**, 62, 22.
- [25] D. Sawai, Y. Tsugane, M. Tamada, T. Kanamoto, M. Sungil, S.-H. Hyon, *J. Polym. Sci., Part B: Polym. Phys.* **2007**, 45, 2632.
- [26] H. Niu, J. Li, Q. Cai, X. Wang, F. Luo, J. Gong, Z. Qiang, J. Ren, *Langmuir* **2020**, 36, 13881.
- [27] R. Liu, B. He, D. Li, Y. Lai, J. Z. Tang, Z. Gu, *Macromol. Rapid Commun.* **2012**, 33, 1061.
- [28] W. Zhang, D. Zhang, X. Fan, G. Bai, Y. Guo, Z. Hu, *RSC Adv.* **2016**, 6, 20761.
- [29] S. Noack, D. Schanzenbach, J. Koetz, H. Schlaad, *Macromol. Rapid Commun.* **2019**, 40, 1800639.
- [30] L. Sun, A. Pitto-Barry, N. Kirby, T. L. Schiller, A. M. Sanchez, M. A. Dyson, J. Sloan, N. R. Wilson, R. K. O'Reilly, A. P. Dove, *Nat. Commun.* **2014**, 5, 5746.
- [31] X. Fan, Z. Wang, D. Yuan, Y. Sun, Z. Li, C. He, *Polym. Chem.* **2014**, 5, 4069.
- [32] Z. Li, D. Yuan, X. Fan, B. H. Tan, C. He, *Langmuir* **2015**, 31, 2321.
- [33] F. K. Wolf, A. M. Hofmann, H. Frey, *Macromolecules* **2010**, 43, 3314.
- [34] X. Hou, Q. Li, A. Cao, *Macromol. Chem. Phys.* **2013**, 214, 1569.
- [35] D. Portinha, F. Boué, L. Bouteiller, G. Carrot, C. Chassenieux, S. Pensec, G. Reiter, *Macromolecules* **2007**, 40, 4037.
- [36] D. Portinha, L. Bouteiller, S. Pensec, A. Richez, C. Chassenieux, *Macromolecules* **2004**, 37, 3401.
- [37] S. H. Kim, J. P. K. Tan, F. Nederberg, K. Fukushima, Y. Y. Yang, R. M. Waymouth, J. L. Hedrick, *Macromolecules* **2009**, 42, 25.
- [38] V. Ladelta, K. Ntetsikas, G. Zapsas, N. Hadjichristidis, *Macromolecules* **2022**, 55, 2832.
- [39] A. Arkanji, V. Ladelta, K. Ntetsikas, N. Hadjichristidis, *Polymers* **2022**, 14, 2431.
- [40] R. M. Michell, A. J. Müller, *Prog. Polym. Sci.* **2016**, 54–55, 183.
- [41] Y. Lan, J. Choi, H. Li, Y. Jia, R. Huang, K. J. Stebe, D. Lee, *Ind. Eng. Chem. Res.* **2019**, 58, 20961.
- [42] W. Yu, M. Inam, J. R. Jones, A. P. Dove, R. K. O'Reilly, *Polym. Chem.* **2017**, 8, 5504.
- [43] S. Karanam, H. Goossens, B. Klumperman, P. Lemstra, *Macromolecules* **2003**, 36, 3051.
- [44] C. Cheng, E. Khoshdel, K. L. Wooley, *Macromolecules* **2005**, 38, 9455.